First imaging of corotating interaction regions using the STEREO spacecraft

A. P. Rouillard,[1,2] J. A. Davies,[2] R. J. Forsyth,[3] A. Rees,[3] C. J. Davis,[2] R. A. Harrison,[2] M. Lockwood,[1,2] D. Bewsher,[2] S. R. Crothers,[2] C. J. Eyles,[2,4] M. Hapgood,[2] and C. H. Perry[2]

Received 28 February 2008; revised 31 March 2008; accepted 17 April 2008; published 31 May 2008.

[1] Plasma parcels are observed propagating from the Sun out to the large coronal heights monitored by the Heliospheric Imagers (HI) instruments onboard the NASA STEREO spacecraft during September 2007. The source region of these out-flowing parcels is found to corotate with the Sun and to be rooted near the western boundary of an equatorial coronal hole. These plasma enhancements evolve during their propagation through the HI cameras' fields of view and only becoming fully developed in the outer camera field of view. We provide evidence that HI is observing the formation of a Corotating Interaction Region (CIR) where fast solar wind from the equatorial coronal hole is interacting with the slow solar wind of the streamer belt located on the western edge of that coronal hole. A dense plasma parcel is also observed near the footpoint of the observed CIR at a distance less than 0.1AU from the Sun where fast wind would have not had time to catch up slow wind. We suggest that this low-lying plasma enhancement is a plasma parcel which has been disconnected from a helmet streamer and subsequently becomes embedded inside the corotating interaction region. **Citation:** Rouillard, A. P., et al. (2008), First imaging of corotating interaction regions using the STEREO spacecraft, *Geophys. Res. Lett.*, *35*, L10110, doi:10.1029/2008GL033767.

1. Introduction

[2] The solar wind is separated into streams of slow wind ($\sim$300 km s^{-1}) and fast wind ($\sim$700 km s^{-1}), the latter often recurring with approximately the equatorial solar rotation period (26–27 days as seen from Earth) [*Neugebauer and Snyder*, 1966]. Fast solar wind streams usually originate in the center of large solar structures called 'coronal holes', which can endure for several months, while slow streams emerge from the vicinity of the helmet streamers in the corona, conventionally imaged by coronagraphs [*Burlaga*, 1995]. Solar rotation will cause an inevitable interaction when slow flow is caught up by fast flow as the solar corona radially expands, leading to the formation of regions of compressed plasma at the interface between the two flows [*Gosling and Pizzo*, 1999]. Such regions of interaction, termed Corotating Interaction Regions (CIRs) if they exhibit a recurrence with the solar rotation period, form on the eastern boundary of the slow solar wind (streamer) belt.

[3] The evolution of CIRs is reasonably well understood following numerical work [*Pizzo and Gosling*, 1994], and a wealth of in-situ observations [*Crooker et al.*, 1999; *Kunow et al.*, 1999, and references therein]. Neither the latitudinal, longitudinal nor the radial evolution of a CIR can be determined continuously from in-situ single spacecraft observations. However cameras observing sunlight which has been Thomson scattered by solar wind electrons can be used to monitor the radial and latitudinal variations of solar wind density variations over several days. The high sensitivity of STEREO Heliospheric Imagers (HI), described in the next section, makes them ideally suited to monitoring the density enhancements created by CIRs.

2. Instruments

[4] The pair of NASA STEREO spacecraft were launched on 26 October 2006 (UT) and inserted into near 1 Astronomical Unit (AU) solar orbits, one leading (STEREO-A) and the other lagging the Earth (STEREO-B). Both spacecraft recede from the Earth by 22.5° per year, as characterised by the spacecraft-Sun-Earth angle [*Kaiser*, 2005]. Each spacecraft carries identical instrumentation including the Sun-Earth Connection Coronal and Heliospheric Investigation (SECCHI) package. SECCHI consists of an Extreme Ultraviolet Imager (EUVI), two coronagraphs (COR-1 and COR-2), and HI. The HI instrument on each STEREO spacecraft comprises two wide-angle imagers, HI-1 and HI-2, which observe in visible light with a band-pass of 630–730 nm and 400–1000 nm, respectively [*Harrison et al.*, 2008]. HI-1 has a 20° square field of view, extending from 4° to 24° in elongation. The 70° by 70° field of view of the outermost HI-2 camera extends from 18.7° to 88.7° elongation. The elongation of a target is defined as the angle between the spacecraft-Sun vector and the spacecraft-target vector. Figure 1a presents a schematic showing the positions of the Sun (S), Earth (E) and STEREO-A (A) spacecraft in the ecliptic plane as viewed from the north for 15 September 2007. The extent in elongation of the fields of view of the HI-1 and HI-2 cameras on the STEREO-A spacecraft (termed HI-1A and HI-2A respectively) in the ecliptic plane are indicated by light and dark shaded areas, respectively. During the interval presented in this paper, images were taken every 40 minutes by HI-1A and every 2 hours by HI-2A. The light detected by HI is sunlight scattered by coronal electrons via Thomson scattering.

[1] Space Environment Physics Group, School of Physics and Astronomy, Southampton University, Southampton, UK.
[2] Space Science and Technology Department, Rutherford Appleton Laboratory, Chilton, UK.
[3] Blackett Laboratory, Imperial College London, London, UK.
[4] Grupo de Astronomia y Ciencias del Espacio, Universidad de Valencia, Valencia, Spain.

0094-8276/08/2008GL033767$05.00

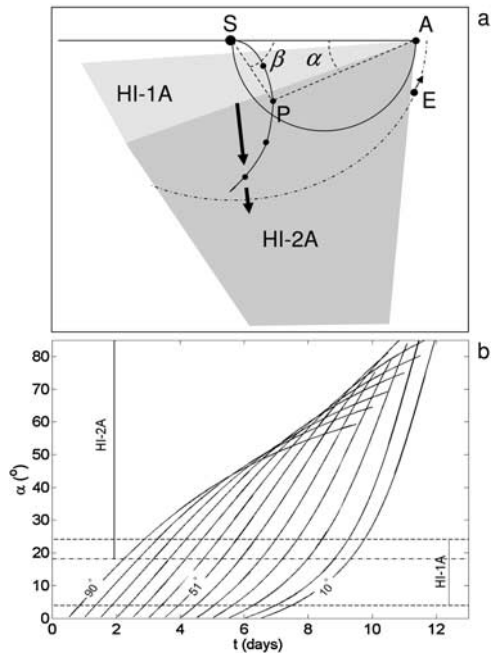

Figure 1. (a) A view of the solar ecliptic plane from the north. (b) $\alpha(t)$ for the equatorial trajectories of a series of structures moving radially outward at the same speed V_r but different β angles as viewed from STEREO-A.

Vourlidas and Howard [2006] showed that electrons on a sphere (the so-called 'Thomson sphere') of diameter the Sun-STEREO segment contribute most effectively to the recorded coronal brightness. The intersection of that sphere with the solar ecliptic is shown in Figure 1a.

3. Tracking Radially Out Flowing Plasma From a Fixed Radial Distance

[5] A series of plasma elements emitted by a single solar source region at 12-hour intervals, and propagating with a radial speed of V_r = 330 km s^{-1} (slow wind), are shown as black dots in Figure 1a. At any instant in time the locus of these plasma elements traces out a spiral with its footpoint at the source region. Each of these plasma elements (such as that labelled P) will have its own fixed longitude of propagation relative to STEREO-A (β) and a varying elongation (α) as it propagates radially outward. An observer located at a constant radial distance from the Sun and measuring the apparent angular distance of a plasma parcel moving at constant radial speed anti-sunward (such as point P) will observe an apparent acceleration/deceleration of that parcel [*Sheeley et al.*, 1999]. The elongation variation [α (t)] of a density front moving radially out with a constant speed (V_r) in the equatorial plane along an observer-Sun-target longitude difference (β) is given by:

$$\alpha(t) = a\tan\left[\frac{V_r t \sin\beta}{r_A(t) - V_r t\cos\beta}\right] \quad (1)$$

where r_A is the heliocentric radial distance of the observer, in this case STEREO-A.

[6] The predicted elongation variation of plasma parcels (with V_r = 330 km s^{-1}) emitted every 12 hours from a source region rotating at the equatorial solar rotation rate of 2.66 × 10^{-6} rad s^{-1}, as seen from STEREO-A, is shown in Figure 1b. The limits in elongation of the HI-1A and HI-2A fields of view in the equatorial plane are shown by horizontal dotted lines. As the source region rotates, the value of β (marked on three of these lines) decreases and the curve of elongation variation changes shape. A plasma parcel propagating in the plane of the sky (here off the eastern limb of the Sun: β = 90°) will appear to decelerate continuously. A parcel propagating along a longitude β = 10° will have a slow apparent speed (small gradient) near the Sun but appear to have much higher speed higher up in the corona (large gradient). Therefore, a series of plasma elements emitted by the same (rotating) source region will leave converging tracks in $\alpha(t)$ plots constructed from STEREO-A HI images.

4. First Observations of a Forming CIRs

[7] Images taken by HI-1/2A on the 9/10 September 2007 showed a region of K-coronal intensity enhancement propagating through both the HI-1A and HI-2A fields of view. Such regions correspond directly to electron density enhancements. A sequence of differenced images from HI-1A (Figures 2a, 2b, and 2c) and HI-2A (Figure 2d) shows the propagation and evolution of this feature. Image

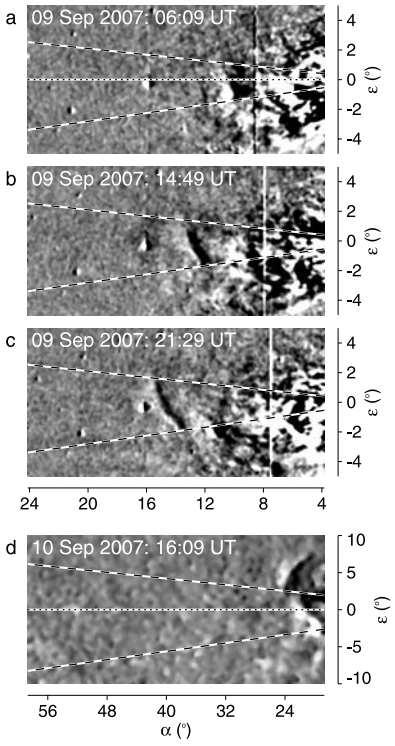

Figure 2. (a, b, c) A sequence of differenced images from HI-1A and (d) HI-2A. The Sun (α = 0°) is to the right hand side of each panel. The extent in elongation (α) and elevation angle (ϵ: out of the plane of Figure 1a) shown for HI-2A is twice that shown for HI-1A. The feature at α = 16° in HI-1A is Mercury. Note that the elongation angles shown are for the central row of each image.

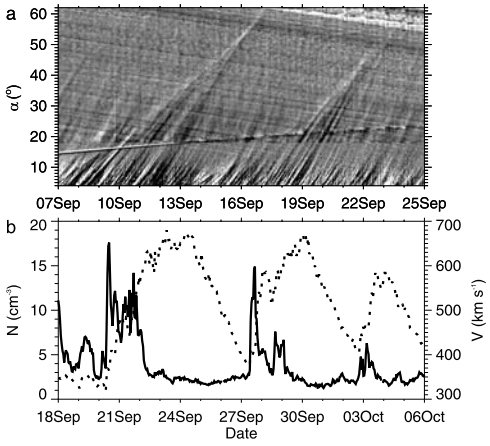

Figure 3. (a) Intensity difference as a function of both elongation, α, and time, t, along the central row of each (differenced) HI-1A and HI-2A image taken between 7 and 25 September 2007. (b) The solar wind density (solid line, left hand axis) and speed (dotted line, right hand axis) observed by ACE from the 18th of September to the 6th of October.

differencing, where each image has subtracted from it the intensity of the previous image, is a commonly used technique for studying the proper motion of faint coronal features [*Sheeley et al.*, 1999].

[8] The plasma parcel associated with the signature seen moving through the HI-1A field of view (Figures 2a, 2b, and 2c), from $\alpha = 10°$ to $\alpha = 15°$ between 6:09 UT and 21:29 UT on 9 September, is estimated to have left the Sun on the 8th. No photospheric activity was reported at this inferred launch time and COR-1 and COR-2 did not observe CME activity. The electron density signature presented in Figure 2 was therefore not driven by CME activity. During this interval, the central row of the HI images (marked in panels a and d of Figure 2) was 2° north of the intersection of the solar equator with the plane of the sky. Lines of constant heliocentric latitudes at +8° and −6°, drawn in the plane of the sky in all panels, bound the latitudinal extent of the plasma parcel; the latitudinal extent of this structure increases only slightly between panels a, b and c (an increase of <+2°). If the structure were to retain the solid angle it covered near the Sun (panel a), radial expansion would force it to expand into a 'pancake' shape (as in fact it does in panel c) at greater coronal heights [*Crooker and Horbury*, 2006]; we conclude therefore that HI-1A is observing the radial expansion of a plasma parcel.

[9] An unusual aspect of this parcel is that it does not show the strong dimming which would be expected from a fall off in density due to radial expansion as it propagates outward. Analysis of the brightness of the star field drifting in the background shows that the sections of HI images presented in Figure 2 are free of optical effects (e.g. vignetting) which could potentially affect the brightness (or here the difference in brightness) of the out-flowing plasma parcel. Panel d, from HI-2A, shows that the structure was still strongly evident in the outer corona and also reveals the presence of a new density enhancement to the north of the parcel tracked in HI-1A, thereby forming an almost semi-circular front in the difference image. This additional dense feature, and the fact that the parcel did not fade but remained a significant feature at greater coronal heights, strongly suggests an electron density increase along the line of sight of the plasma parcel. A similar out-flowing parcel was observed in HI-1/2A 26 days earlier on 13 August which indicates that it was recurrent.

[10] Figure 3a presents the intensity difference, as a function of both elongation and time, from HI on STEREO-A. The central row from each differenced HI-1A and HI-2A image (shown as dotted lines in Figures 2a and 2d) taken between 7 and 25 September 2007 is used to construct Figure 3. The signature in Figure 3a of the density enhancement imaged in Figure 2 is the first of the family of converging tracks formed between 8 and 12 September. These tracks are strikingly similar to the pattern of converging curves shown for plasma elements emitted by a corotating source region (Figure 1b). The 4-day period over which the successive density enhancements appear in HI-1A corresponds to the time taken for a source region to rotate from the Eastern limb to align with the Sun-STEREO line as shown in Figure 1b. The elongation variation of the plasma parcel shown in Figure 2 fits best equation 1 for values of V_r of 270 km s^{-1} and β of 84. This plasma parcel is therefore propagating from coronal height of ~0.07 AU from Sun-center to a distance of ~0.45 AU between $\alpha = 4°$ and $\alpha = 24°$. The direction of propagation of the plasma parcel is marked by black arrows in Figure 1a; the parcel is moving rapidly away from the Thomson sphere during its propagation from HI-1A to HI-2A which would cause a reduction in its brightness; despite this a new density enhancement is observed in near $\alpha = 24°$ which was not apparent at smaller elongations. Another family of converging tracks formed between 16 and 20 September.

[11] Many tracks in Figure 3a extend from the inner corona ($\alpha < 10°$) and are likely to be initially plasma parcels emitted from a corotating source (such as the parcel observed in Figures 2a, 2b, and 2c). The expected dimming of the parcel in Figure 2 due to radial expansion is not observed. We suggest two possible reasons for this: (i) a rapid increase in solar wind speed could be driving plasma compression inside the slower parcel or (ii) due to its propagation angle ($\beta \sim 84°$), HI is observing the dense parcel increasingly along the Parker spiral during its propagation and therefore a brightness increase is caused by more plasma contributing along the line of sight. We note that if the second effect was dominant then plasma parcels propagating at small angles to the Sun-STEREO line would disappear progressively during their outward propagation as HI would increasingly observe across the spiral; this effect is not seen in Figure 3a.

[12] Figure 3b shows in-situ plasma density and speed measurements [*McComas et al.*, 1998] made by the Advanced Composition Explorer (ACE), as solid and dotted black lines respectively, for the period extending from 18 September to 6 October. ACE is located at an elongation of approximately $\alpha = 90°$ (1 AU). If the 8–12 September tracks were CIR-associated, we estimate, using equation 1, that a density enhancement should reach ACE on the 21st. A CIR passage (a density enhancement on a leading edge of a wind speed rise) was indeed observed by ACE on the 20–22 September. In the same way, the 16th–20th family of tracks were followed by increased density at ACE on

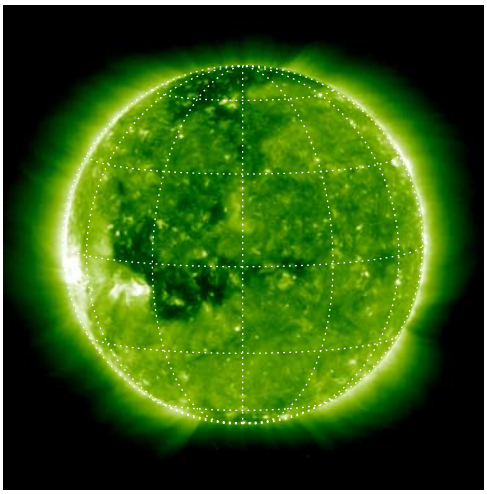

Figure 4. Extreme ultraviolet image of the solar corona, taken at 195 Å. Lines of constant heliocentric latitudes and longitudes are overlaid on the image.

27 September. Similar patterns were observed both 52 days and 26 days earlier.

[13] Figure 4 is an image taken by EUVI on STEREO-A seven days after the launch of the plasma parcel observed in Figure 2; this is the time required for solar rotation to bring coronal features on the east limb into the field of view of EUVI. The image reveals the presence of a coronal hole extending into the equatorial regions. As discussed above, coronal holes are central to CIR formation. The predictions made by the ENLIL 3-D MHD numerical model of the solar wind [*Odstrčil and Pizzo*, 1999], available at the Community Coordinated Modelling Center (CCMC) web-based interface, confirm that fast solar wind (>600 km s^{-1}) was emitted by this equatorial coronal hole and that a CIR was propagating through HI-1/2A fields of view at the time.

5. Discussion and Conclusions

[14] In this paper, a dense and therefore, bright plasma feature was tracked in HI images (Figure 2). Its height versus time track was consistent with that of a parcel moving along a $\beta \sim 84°$ and at $V_r \sim 270$ km s^{-1}. The β and V_r values allow us to determine the source region of the parcel which is found to be the western edge of an equatorial coronal hole. Elongation versus time plots showed that this propagating solar wind structure was part of a series of converging events seen over a 4–6 day interval through the inner HI-1A camera and then in the outer HI-2A camera. A similar set of tracks is observed one and two solar rotations earlier indicating that the structure is recurrent. Assuming that this track is part of a CIR appears valid, as its estimated arrival time at Earth coincides with the passage of a CIR monitored by the ACE plasma instruments. Moreover numerical modelling predicts the passage of a CIR in the HI images at the same time. The brightness variation of the out-flowing plasma parcel shown in this paper is a complicated convolution of three observational effects discussed here: the level of compression of plasma inside the interaction region, the position of the parcel relative to the Thomson sphere and the distribution of density inside the Parker spiral. Future work should attempt to disentangle these three effects.

[15] There is already evidence of signatures associated with this corotating structure near the sunward edge of HI-1A and future work should concentrate on tracking these structures systematically using the COR-1 and COR-2 coronagraphs. To date the only observations of 'non-CME associated blobs' have been those tracked in the SOHO coronagraphs [*Wang et al.*, 1999] which were associated with parts of the helmet streamers which presumably had been disconnected via magnetic reconnection. We therefore suggest the possibility that the density structure shown in Figures 2a, 2b, and 2c might be such a 'blob' disconnected from the streamers and subsequently swept inside the CIR.

[16] **Acknowledgments.** We thank the two referee for their constructive comments. We thank the ACE SWEPAM team and CCMC for providing the solar wind in-situ and the modelling data respectively. The STEREO/SECCHI data are produced by a consortium of RAL (UK), NRL (USA), LMSAL (USA), GSFC (USA), MPS (Germany), CSL (Belgium), IOTA (France) and IAS (France) and stored by WDC Chilton.

References

Burlaga, L. F. (1995), *Interplanetary Magnetohydrodynamics*, 1st ed., Oxford Univ. Press, New York.

Crooker, N. U., and T. S. Horbury (2006), Solar imprint on ICMEs, their magnetic connectivity, and heliospheric evolution, *Space Sci. Rev.*, *123*, 93.

Crooker, N. U., et al. (1999), CIR morphology, turbulence, discontinuities, and energetic particles—Report of working group 2, *Space Sci. Rev.*, *89*, 179.

Gosling, J. T., and V. J. Pizzo (1999), Formation and evolution of corotating interaction regions and their three dimensional structure, *Space Sci. Rev.*, *89*, 21.

Harrison, R. A., et al. (2008), First imaging of coronal mass ejections in the heliosphere viewed from outside the Sun-Earth line, *Sol. Phys.*, *247*(1), 171.

Kaiser, M. L. (2005), The STEREO mission: An overview, *Adv. Space Res.*, *36*, 1483.

Kunow, H., B. Heber, and J. A. Simpson (1999), Corotating interaction regions at high latitudes, *Space Sci. Rev.*, *83*, 215.

McComas, D. J., et al. (1998), Solar Wind Electron Proton Alpha Monitor (SWEPAM) for the Advanced Composition Explorer, *Space Sci. Rev.*, *86*, 563.

Neugebauer, M., and C. W. Snyder (1966), Mariner 2 observations of the solar wind: 1. Average properties, *J. Geophys. Res.*, *71*, 4469.

Odstrčil, D., and V. J. Pizzo (1999), Distortion of the interplanetary magnetic field by three-dimensional propagation of coronal mass ejections in a structured solar wind, *J. Geophys. Res.*, *104*, 28,225.

Pizzo, V. J., and J. T. Gosling (1994), 3-D simulation of high-latitude interaction regions: Comparison with Ulysses results, *Geophys. Res. Lett.*, *21*, 2063.

Sheeley, N. R., et al. (1999), Continuous tracking of coronal outflows: Two kinds of coronal mass ejections, *J. Geophys. Res.*, *104*, 24,739.

Vourlidas, A., and R. A. Howard (2006), The proper treatment of coronal mass ejection brightness: A new methodology and implications for observations, *Astrophys. J.*, *642*(2), 1216.

Wang, Y.-M., et al. (1999), Streamer disconnection events observed with the LASCO coronagraph, *Geophys. Res. Lett.*, *26*, 1349.

D. Bewsher, S. R. Crothers, J. A. Davies, C. J. Davis, C. J. Eyles, M. Hapgood, R. A. Harrison, M. Lockwood, C. H. Perry, and A. P. Rouillard, Space Science and Technology Department, Rutherford Appleton Laboratory, Chilton OX11 0QX, UK. (alexisrouillard@yahoo.co.uk)

R. J. Forsyth and A. Rees, Blackett Laboratory, Imperial College London, London SW7 2BZ, UK.